Genetic Control of Genomic Alterations Induced in Yeast by Interstitial Telomeric Sequences

Anthony Moore,*,† Margaret Dominska,*,† Patricia Greenwell,*,† Anna Y. Aksenova,‡ Sergei Mirkin,§ and Thomas Petes*,‡,1

*Department of Molecular Genetics and Microbiology and †University Program in Genetics and Genomics, Duke University Medical Center, Durham, North Carolina 27710, ‡Laboratory of Amyloid Biology, St. Petersburg State University, 199034, Russia, and §Department of Biology, Tufts University, Medford, Massachusetts 02155

ORCID ID: 0000-0003-4890-8002 (T.P.)

ABSTRACT In many organisms, telomeric sequences can be located internally on the chromosome in addition to their usual positions at the ends of the chromosome. In humans, such interstitial telomeric sequences (ITSs) are nonrandomly associated with translocation breakpoints in tumor cells and with chromosome fragile sites (regions of the chromosome that break in response to perturbed DNA replication). We previously showed that ITSs in yeast generated several different types of instability, including terminal inversions (recombination between the ITS and the "true" chromosome telomere) and point mutations in DNA sequences adjacent to the ITS. In the current study, we examine the genetic control of these events. We show that the terminal inversions occur by the single-strand annealing pathway of DNA repair following the formation of a double-stranded DNA break within the ITS. The point mutations induced by the ITS require the error-prone DNA polymerase ζ. Unlike the terminal inversions, these events are not initiated by a double-stranded DNA break, but likely result from the error-prone repair of a single-stranded DNA gap or recruitment of DNA polymerase ζ in the absence of DNA damage.

KEYWORDS recombination; mutagenesis; interstitial telomeric repeats; DNA replication; inversions

THE ends (telomeres) of the chromosomes have several properties that distinguish them from most genomic sequences. In most organisms, telomeres are replicated by the telomerase ribonucleoprotein complex (Greider and Blackburn 1985). In addition, telomeres have a structure (the cap) that distinguishes the natural end of the chromosome from ends produced by DNA damage, preventing telomere–telomere fusions (Wellinger and Zakian 2012). One last unusual property of the telomeres in some organisms (including *Saccharomyces cerevisiae*) is their ability to transcriptionally silence genes located nearby (Gottschling *et al.* 1990).

In yeast, as in most organisms, the telomeric sequences are simple repeats (Wellinger and Zakian 2012). Unlike most organisms, in *S. cerevisiae*, the repeat is imperfect of the form $C_{1-3}A/G_{1-3}T$. Wild-type strains have a double-stranded region of this sequence of ~300 bp, and a single-stranded 3′ $G_{1-3}T$ "tail" of ~15 bases (Wellinger and Zakian 2012). There are a large number of proteins that bind directly to telomeric DNA or indirectly to the telomere by binding to other proteins including Rap1p, Cdc13p, Stn1p, Ten1p, Rif1p, Rif2p, Sir2p, Sir3p, Sir4p, Yku70p, Yku80p, Rfa1p, Rfa2p, Rfa3p, Est1p, Est2p, and Est3p, as well as the telomerase RNA TLC1 (Kupiec 2014). In addition to the proteins that usually reside at the telomere, there are proteins that have a more transient interaction [such as Tel1p/Mec1p and the Mre11p/Rad50p/Xrs2p (MRX) complex], present at certain times in the cell cycle or when the telomeres shorten below a critical length.

In many organisms, telomeric sequences can be found embedded within the chromosome. These interstitial telomeric sequences (ITSs) were first detected by *in situ* hybridization (Meyne *et al.* 1990; Azzalin *et al.* 1997) and, subsequently, by DNA sequencing. The human genome contains > 100 ITSs that have a minimum repeat length of four repeats (Azzalin *et al.* 2001). Two lines of evidence

doi: https://doi.org/10.1534/genetics.118.300950
Manuscript received October 9, 2017; accepted for publication March 27, 2018; published Early Online April 2, 2018.
Available freely online through the author-supported open access option.
Supplemental material available at Figshare: https://doi.org/10.25386/genetics.6013667.
[1]Corresponding author: Department of Molecular Genetics and Microbiology, Duke University School of Medicine, Duke University Medical Center, 213 Research Drive, Durham, NC 27710. E-mail: tom.petes@duke.edu

suggest that ITSs may represent breakage-prone sites in the mammalian genome (Lin and Yan 2008). First, ITSs are significantly overrepresented in translocation breakpoints observed in tumor cells. Second, fragile sites (regions of the genome prone to breakage in conditions of DNA replication stress) are enriched for ITSs.

We have recently begun to investigate the effect of ITSs on genome stability in the yeast *S. cerevisiae* (Aksenova *et al.* 2013, 2015). Using a system that will be described in detail in the *Results* section, we showed that ITSs stimulated two types of genomic alterations: point mutations near the site of the ITS insertion and chromosome rearrangements. The most common rearrangement was a terminal inversion between the ITS and the true chromosome telomere. In our 2013 study, we restricted our analysis to a wild-type strain. In the current study, we examine the rates of ITS-induced genomic alterations in strains with mutations affecting DNA repair/recombination and telomere metabolism. We show that ITS-induced point mutations require the error-prone DNA polymerase ζ and are not initiated by a double-strand DNA break (DSB). In contrast, the terminal inversions are likely initiated by a DSB and are repaired by a single-strand annealing (SSA) pathway.

Materials and Methods

Yeast strains and plasmids

The genotypes and details of construction for the strains used in this study are in Supplemental Material, Table S1, and the primers used in strain construction/strain analysis are in Tables S2 and S3. Most strains are derivatives of the previously described haploid SMY749 (Aksenova *et al.* 2013). This strain is isogenic with the commonly-used lab strain S288c and has the genotype: *MAT***a** *leu2-Δ1 trp1-Δ63 ura3-52 his3-200 ade2Δ*::*kanMX4 III*(*75594–75641*)::*URA3-Int-*(*TGTGTGGG*)$_{15}$*-TRP1*; the reporter gene with the ITS is located on chromosome III (Figure 1A). As described in Table S1, we isolated a derivative of SMY749 (PG329) in which we replaced *ura3-52* with a drug resistance marker (*natMX4*). Mutant derivatives of PG329 lacking various genes involved in DNA repair, recombination, or telomere elongation were also generated (Table S1). The deletions were constructed by standard procedures using PCR fragments containing drug resistance markers; these fragments were obtained by amplifying plasmids containing either *hphMX4* or *natMX6* as described in Table S1. All insertions and deletions were confirmed by PCR using primers described in Table S3.

Yeast media

In most experiments, standard media were used (Guthrie and Fink 1991). Medium with 5-fluoro-orotate (5-FOA) contained 1 g of 5-FOA and 40 mg of uracil per liter in synthetic dextrose (SD) complete (SD-complete) medium. Medium containing 5-FOA and canavanine had the same amount of uracil and 5-FOA, but contained 120 mg of canavanine per liter; in addition, the medium lacked arginine. The medium used to check for silencing of *TRP1* expression was SD-tryptophan medium containing 70 mg of nicotinamide per liter. Sporulation medium was standard (Guthrie and Fink 1991).

Measurements of rates of genetic alterations in strains with URA3-Int-(TGTGTGGG)$_{15}$-TRP1 on chromosome III

We measured several types of genetic instability in our analysis. In most of the studies, we first determined the rate of 5-FOA^R (5-FOA-resistant) derivatives in strains that contained the *URA3-Int-*(*TGTGTGGG*)$_{15}$*-TRP1* reporter gene integrated on chromosome III. For these experiments, the strains were streaked on rich growth medium (YPD) and allowed to form colonies at 30°. Individual colonies were then grown as small patches on YPD for 1 day. Individual patches were resuspended in water and various dilutions were plated to SD-complete or SD medium containing 5-FOA. In each experiment, we examined 15–20 independent colonies and we performed two separate experiments for each strain. Based on the total number of cells in the patch and the number of 5-FOA^R derivatives, we calculated a rate of formation of 5-FOA resistance for each strain using the method of the median (Lea and Coulson 1949).

We found three classes of 5-FOA^R derivatives: class 1 (point mutations within the *URA3* reporter), class 2 (terminal inversions involving the ITS), and class 3 (uncharacterized chromosome rearrangements). For each strain, we examined at least 20 independent 5-FOA^R derivatives using a series of tests. First, we performed PCR with all the isolates using the primers UIRL1/UIRL2 and UIRL2/CHR413R (Figure 1A). UIRL1/UIRL2 flank the ITS and produce a PCR product if there is a point mutation (class 1). The UIRL2 and CHR413R primers produce a PCR product if there is a terminal inversion (class 2). Failure to detect a PCR product with either set of primers indicates class 3. Second, we tested whether the 5-FOA^R derivatives failed to grow in medium lacking tryptophan but could grow in medium lacking tryptophan that contained nicotinamide. Because terminal inversions result in a larger insertion of telomeric sequences near the *TRP1* gene, the *TRP1* gene is silenced epigenetically, and this silencing is reversible by nicotinamide (Aksenova *et al.* 2013). In contrast, most class 3 strains were Trp$^-$, but the tryptophan requirement could not be reversed with nicotinamide. Using the criteria described above, we found that $>$ 90% of the strains were classes 1 and 2, with class 3 representing a minor fraction. We calculated the rates of formation of classes 1 and 2 by multiplying the proportion of these events among the 5-FOA^R derivatives by the rate of 5-FOA^R.

Determination of 95% confidence limits on rate measurements

For the calculation of 95% confidence limits (CL) on the median rates of 5-FOA^R derivatives, we used the ranking method described previously (Wierdl *et al.* 1996). The procedure for

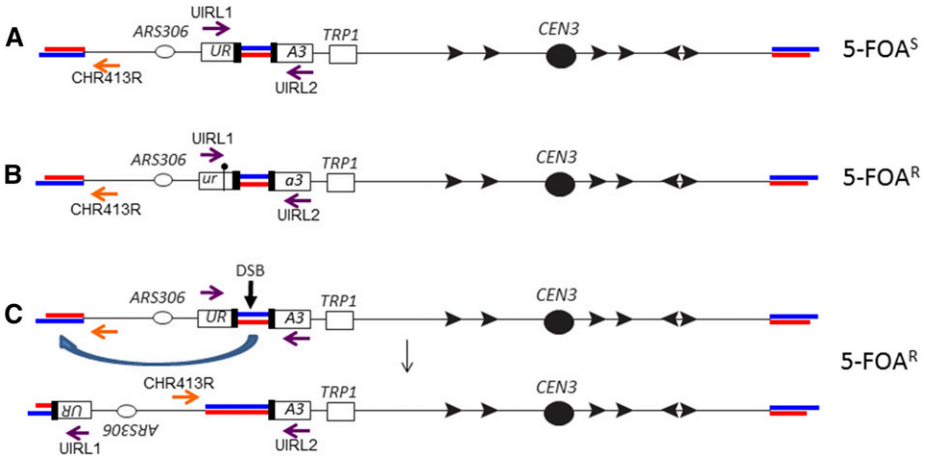

Figure 1 Genetic system used to detect genomic alterations induced by ITSs. Telomeres and ITSs are shown as paired red and blue lines, with red and blue representing the CA-rich and GT-rich strands, respectively. The top strand is shown with the 5′ end on the left side. Only telomeric repeats with the GT-rich strand on the 3′ end have telomere function. Black arrows indicate Ty elements, and purple and orange arrows indicate the orientations and positions of primers used to diagnose genomic alterations. The ITS is replicated by forks initiated at *ARS306*. The figure is not drawn to scale. (A) Reporter gene used in our study (Aksenova *et al.* 2013). The ITSs are inserted within an intron embedded with *URA3*; the length of the ITS is 120 bp, representing 15 copies of an 8-bp repeat (TGTGTGGG). Strains with this reporter are Ura$^+$ Trp$^+$, and we selected 5-FOA^R derivatives to detect genomic alterations. (B) Point mutations induced by the ITSs. These derivatives are Ura$^-$ Trp$^+$ and have a PCR fragment of the expected size when the purple primers flanking the ITS are used (UIRL1 and UIRL2 in Table S2). Sequencing of PCR fragments demonstrates that these events are associated with a point mutation in the *URA3* coding sequences flanking the ITS. (C) Terminal inversions induced by the ITSs. In this class, no PCR fragment is found with the purple primers, but a PCR fragment is observed using the orange primer (Chr3_413R in Table S2) and the centromere-proximal purple primer (UIRL2). In addition to the 5-FOA^R phenotype, most of this class are Trp$^-$, as a consequence of epigenetic silencing of *URA3* caused by the longer region of telomeric repeats resulting from the inversion; the Trp$^-$ phenotype is reversed when the cells are analyzed on plates lacking tryptophan but containing the Sir2p-inhibitor nicotinamide. 5-FOA^R, 5-FOA-resistant; DSB, double-strand break; ITS, interstitial telomeric sequence.

determining the 95% CL of the rates of class 1 and class 2 isolates is more complex because both the CLs on the rates of 5-FOA^R and on the proportions of each class must be considered. The 95% limits on the proportions of each class were calculated using the Vassarstat website (http://vassarstats.net). If the rate of class 1 or class 2 events is Q, the rate of 5-FOA^R is A, and the proportion of class 1 or class 2 events is B, we calculate the error (confidence interval) for Q (δQ) by the equation:

$$\delta Q = Q \times \sqrt{[(\delta A/A)^2 + \delta B/AB)^2]}$$

(http://ipl.physics.harvard.edu/wp-uploads/2013/03/PS3_Error_Propagation_sp13.pdf).

To illustrate the method used to calculate the 95% CL of class 1 and class 2 events, we will use the data from the wild-type strain PG329 as an example. The median rate of 5-FOA^R derivatives was 18.6×10^{-7} (95% CL of 14–24 $\times 10^{-7}$); the median rate and the 95% CL on the rate were calculated as described by Wierdl *et al.* (1996). Of 107 5-FOA^R mutants examined, 52 had point mutations; this proportion is 0.486 (95% CL of 0.39–0.58). The 95% limits on the proportions were calculated using the "The Confidence Interval of a Proportion" section of the Vassarstat website. The rate of point mutations was $18.6 \times 10^{-7} \times 0.486 = 9.0 \times 10^{-7}$. To obtain the upper CL limit on this rate, we used the following protocol. First, (step 1) subtract the median rate of 5-FOA^R from the rate representing the upper 95% CL (24×10^{-7}–$18.6 \times 10^{-7} = 5.4 \times 10^{-7}$); (step 2) divide the value of step 1 by the median rate of 5-FOA^R [$(5.4 \times 10^{-7})/(18.6 \times 10^{-7}) = 0.30$]; and (step 3) square the value obtained in step 2; [$(0.30)^2 = 0.09$]. For steps 4–6, perform the comparable steps with the data for the proportion: (step 4) 0.58–0.486 = 0.094; (step 5) (0.094)/(0.486) = 0.19; and (step 6) $(0.19)^2 = 0.036$. For step 7, add the values calculated for steps 3 and 6 (0.09 + 0.036 = 0.126). For step 8, take the square root of the value calculated for step 7 [$(0.126)^{1/2} = 0.35$]. For step 9, multiply the value obtained in step 8 by the rate of point mutations ($0.35 \times 9.0 \times 10^{-7} = 3.15 \times 10^{-7}$). The upper 95% CL is equal to the median rate of the point mutations plus the value calculated in step 9 ($9.0 \times 10^{-7} + 3.15 \times 10^{-7}$ or 12.2×10^{-7}). Performing comparable steps for the lower 95% CL, we calculate a value of 6.1×10^{-7}. In summary, for point mutations, the rate is 9.0×10^{-7} (95% CL of 6.1–12.2 $\times 10^{-7}$). Similar calculations for the terminal inversions yield a rate of 9×10^{-7} (CL of 5.9–12 $\times 10^{-7}$). These values and those for the mutant strains are in Table 1.

Data availability

All data and strains used in this study are available on request. Supplemental material available at Figshare: https://doi.org/10.25386/genetics.6013667.

Results

Experimental system

The system used by Aksenova *et al.* (2013) and in the present study is shown in Figure 1A. The reporter *URA3* gene has an intron with 15 copies of the yeast telomeric repeat (TGTGTGGG). This gene (*URA3*::*Int* $(TGTGTGGG)_{15}$) was inserted on chromosome III near *ARS306* ~70 kb from the left end. We determined the mutation rate of this gene by measuring the frequency of 5-FOA^R, a phenotype associated with *ura3*

Table 1 Rates of *ura3* point mutations and terminal inversions in strains of different genotypes

Genotype[a]	Rate of *ura3* point mutations (class 1) ($\mu \times 10^{-7}$)	Rate of class 1 normalized to wild-type	Rate of terminal inversions (class 2) ($\mu \times 10^{-7}$)	Rate of class 2 normalized to wild-type
Wild-type	9.0 (6.1–12)	1	9 (5.9–12)	1
*elg1*Δ	11 (5.5–19)	1.2	5.2 (2.1–10)	0.6
*exo1*Δ	18 (11–25)	1.9*	15 (9.1–22)	1.2
*lig4*Δ	9.2 (5.4–13)	1	9.2 (5.4–13)	1
*mms2*Δ	6.4 (3.4–11)	0.71	9.7 (5.4–13)	1.1
mre11Δ	1.1 (0.6–3.6)**	0.12	1.3 (0.7–4.2)**	0.14
mre11-H125N	2.9 (1.4–4.9) **	0.32	7.5 (4.5–9.8)	0.83
msh2Δ	9 (6.2–13) [0.98]	0.98	0.6 (0.2–1.4)**	0.07
*msh6*Δ	8.7 (5.5–14)	0.97	7.8 (4.8–13)	0.9
*mus81*Δ	14 (8.2–22)*	1.5	6.9 (3.8–11)	0.77
rad1Δ	14 (8.2–22)*	1.5	1.4 (0.4–3.0)**	0.15
*rad18*Δ	5.6 (2.2–9.1)*	0.62	8.9 (3.5–12)	1
rad50Δ	3.1 (2.0–4.1)**	0.34	0.9 (0.4–1.8)**	0.1
rad51Δ	19 (12–26)*	2.1	13 (7.4–20)*	1.5
rad52Δ	*36 (30–58)***	4	1 (0.07–6)*	0.1
rad59Δ	13 (8.9–19)*	1.4	2.2 (0.9–4.7)**	0.25
rev3Δ	0.9 (0.4–1.9)**	0.1	4.4 (3.1–7.2)*	0.49
*rif1*Δ	11 (8.3–22)	1.2	12 (4.7–16)	1.3
rrm3Δ	11 (7.6–15)	1.2	2.1 (0.8–4.4)**	0.24
sae2Δ	3.4 (1.4–6.6)*	0.37	12 (7.1–18)	1.3
sgs1Δ	14 (6.3–23)*	1.6	1.3 (0.1–3.8)**	0.2
sir2Δ	3.2 (1–8) [0.4]*	0.4	*27 (20–34)***	3
sir3Δ	0.55 (0.1–1.9)**	0.06	8.3 (6.3–11)	0.92
*sml1*Δ	12 (6.8–19)	1.3	11 (6.3–18)	1.3
srs2Δ	7.1 (4.6–9.4)	0.77	2.0 (1.0–3.3)**	0.22
*tel1*Δ	17 (11–26)*	1.9	23 (11–33)*	2.6
tof1Δ	3.4 (1.7–6.8)*	0.38	2. (1.7–6.8)*	0.38
tof1Δ mre11Δ	5.7 (4.1–7.1)*	0.3	0 (0–0.8)**	0
*top1*Δ	6.1 (3.8–8.7)	0.67	7.2 (4.6–10)	0.8

Rates were calculated as described in the text. 95% confidence limits are shown in parentheses and the rates normalized to the wild-type rate are shown in squared brackets. Single asterisks indicate that the rate is outside of the 95% confidence limits of the wild-type strain, and double asterisks show that the rates of the mutant and wild-type strain do not overlap. For rates with double asterisks, underlines and italics indicate whether the rate is higher or lower than the comparable wild-type rates, respectively.

[a] Strain names for the various genotypes listed from top to bottom are: PG329, MD651, MD653, MD687, AM17, AM13, MD740, AM24, MD659, MD658, MD689, AM26, MD691, MD655, MD649, MD686, AM12, MD647, AM14, MD708, MD688, MD657, MD736, MD646, AM15, MD644, MD674, MD734, and MD661. Genotypes shown in bold are the ones used most extensively in developing our models for the genetic regulation of interstitial telomeric sequence-induced instability.

mutant strains (Boeke *et al.* 1984). The purple and orange arrows in Figure 1 show the location of primers that were used to diagnose the genomic alterations (as described in the section below).

The rate of 5-FOA^R was elevated by the ITS ~100-fold compared to the rate for an intron-containing *URA3* in the same location without the ITS (Aksenova *et al.* 2013). About half of these Ura$^-$ derivatives had point mutations in *ura3* (Figure 1B) and the remainder had chromosome alterations of several different types. A common chromosome alteration was a terminal inversion of the sequences located between the ITS and the true telomere; we assume that this rearrangement was initiated by a DSB within the ITS (Figure 1C). We previously observed chromosome rearrangements in addition to the terminal inversion; some of these rearrangements involved an interaction between Ty elements located near the ITS on chromosome III and the Ty insertion in the *ura3* gene (*ura3-52*) on chromosome V (Aksenova *et al.* 2013). To avoid getting this class of rearrangement, in the current study, we deleted the *ura3-52* allele. In this strain (PG329), as described below, almost all (> 90%) of the 5-FOA^R derivatives had point mutations (class 1) or terminal inversions (class 2).

ITS-induced genomic alterations in the wild-type strain PG329

The rate of 5-FOA^R in the wild-type strain was 1.9×10^{-6} /division (95% CL of 1.4–2.4 $\times$ 10^{-6}) (Table 1), 52-fold higher than the rate in an isogenic strain (AM21) with the same *URA3* reporter gene lacking an ITS [3.5×10^{-8} (1.7–23 $\times$ 10^{-8})]. To confirm that ITS-induced mutagenesis in PG329 occurred locally rather than on a genome-wide basis, we examined mutation rates at the *CAN1* locus in PG329 and in a strain lacking the ITS insertion (SMY803). The mutation rate to canavanine resistance was very similar in the two strains: 2.2×10^{-7}/division (CL 1.6–3.3 $\times$ 10^{-7}) in PG329 and 1.4×10^{-7}/division (CL 1.4–3.9 $\times$ 10^{-7}) in SMY803.

Three classes of genomic alterations were found among 107 independent 5-FOA^R derivatives that were examined. Class 1 strains (52 of 107) were Trp$^+$ on standard omission medium, and genomic DNA from these strains produced a PCR fragment when examined using primers UIRL1 and

UIRL2 flanking the ITS (shown in Figure 1B). The *ura3* genes from 29 class 1 strains were sequenced and all had mutations in the coding sequence flanking the ITS insertion (Figure S1). Genomic DNA samples from class 2 strains (51 of 107) had a PCR fragment when analyzed with the primers CHR413R and UIRL2 (Figure 1C), indicating that these strains had a terminal inversion. These strains were Trp^- on standard omission medium, but Trp^+ on medium lacking tryptophan but containing nicotinamide; nicotinamide is a drug that reverses silencing induced by telomeric repeats (Bitterman *et al.* 2002). These phenotypes are also diagnostic of a terminal inversion because such inversions resulted in a larger insertion of telomeric sequences near the *TRP1* gene, producing an epigenetic silencing of *TRP1* (Aksenova *et al.* 2013). Class 3 strains are Trp^- on standard omission medium and fail to produce a PCR product with either set of primers used to diagnose class 1 and 2 strains. Since class 3 strains represent $< 10\%$ of the events (Table S4), we did not further characterize them. Based on our previous study (Aksenova *et al.* 2013), most of the class 3 strains likely reflect recombination between Ty elements located near *URA3*::*Int* $(TGTGTGGG)_{15}$ and other Ty elements in the genome. In summary, the ITS-induced genomic alterations in PG329 were approximately equal numbers of point mutations and terminal inversions, with a much lower frequency of other types of events.

Genetic regulation of ITS-induced genomic changes: general considerations

We constructed a series of strains isogenic with PG329 except for mutations affecting various pathways of DNA repair, DNA replication, and telomere metabolism. For each strain, we measured 5-FOA^R in two independent experiments, each involving at least 15 cultures. At least 20 independent 5-FOA^R isolates were classified as class 1, 2, or 3 by the tests described above. Based on these values, we calculated the rates of formation of class 1 and 2 events for each mutant strain (Table 1).

It is likely that both class 1 and 2 events are initiated by a DNA lesion (DSB or single-stranded nick) or a stall of the DNA replication fork at the ITS, since the ITS does not result in a mutator phenotype at other genomic loci; the nature of the initiating event may be different or the same for class 1 and 2 events. Following the initiating event, the subsequent mechanisms that produce class 1 and 2 events are likely quite different, although some of the same enzymes may be involved. The frequencies of the two classes of events can be regulated either at the level of initiation or at subsequent steps.

The genes that we examined for their effects on ITS-mediated instability and the functions regulated by the proteins encoded by these genes are in Table 2. We analyzed proteins involved in regulating the stability of the replication fork (Rrm3p, Sgs1p, Srs2p, and Tof1p), since previous studies showed that some genome-destabilizing sequences resulted from problems related to DNA replication (Anand *et al.* 2012; Shah *et al.* 2012). Since the binding of sequence-specific proteins can affect the frequency of fork stalling, we analyzed mutants affecting telomere-binding proteins (Rif1p, Sir2p, Sir3p, and Tel1p). We studied mutations affecting the repair of DSBs by homologous recombination (HR) (Exo1p, Mre11p, Mus81p, Rad1p, Rad50p, Rad51p, Rad52p, Rad59p, and Sae2p) and by nonhomologous end-joining (Lig4p), since terminal inversions are likely to reflect a recombinational interaction between the ITS and the telomere. We also examined mutants that affect the ratio of error-free (Mms2p and Rad18p) to error-prone (Rev3p) postreplication repair, since such mutants could affect the relative frequencies of the class 1 and 2 events. Lastly, we examined strains with defective mismatch repair (Msh2p and Msh6p) to determine whether the class 1 mutations were subject to mismatch repair.

Genetic regulation of class 1 events

In some previous studies of mutations induced by trinucleotide repeats or palindromic sequences, the induction of mutants in nearby sequences was dependent on the error-prone DNA polymerase ζ (Shah and Mirkin 2015). We found that the *rev3* mutation (eliminating the catalytic subunit of DNA polymerase ζ) reduced the rate of class 1 events ~10-fold (Table 1). DNA polymerase ζ is recruited to the sites of DNA damage as well as stalled replication forks that lack overt damage (Northam *et al.* 2010, 2014; Makarova and Burgers 2015). ITSs in yeast were previously associated with both stalled replication forks and a low frequency of DSB formation (Anand *et al.* 2012; Goto *et al.* 2015).

To determine whether the class 1 events were associated with repair of a DSB, we examined the length of the ITSs in strains with a class 1 event. The rationale for this approach is shown in Figure 2A. In our previous study of point mutations induced by a $(GAA)_N$ tract, we found that $> 80\%$ mutations were associated with a loss of repeats from the $(GAA)_N$ tract. Since these tracts also resulted in high levels of DSBs (Tang *et al.* 2011), to account for these findings, we suggested that the mutagenesis was initiated by a DSB within the GAA tract, followed by processing of the broken ends by 5′–3′ degradation (Tang *et al.* 2013). Reannealing of these broken ends, and repair of the two single-stranded gaps by DNA polymerase ζ, would result in an elevated rate of mutations in the linked reporter gene and a decrease in the length of the GAA tract (Figure 2A). To determine whether a similar mechanism explained the ITS-mediated class 1 events, we examined the length of the ITS in 37 strains that had a class 1 event. No alterations were observed in 34 strains, two gained one copy of the telomeric repeat, and one gained three copies. These results argue that class 1 events are not likely to reflect repair of an ITS-associated DSB. Alternatives are that the class 1 events result from the recruitment of error-prone DNA polymerase to ITS-associated single-stranded gaps (Figure 2B) or from the recruitment of the error-prone polymerase to a slow-moving or stalled replication fork in the absence of DNA damage (Figure 2C).

Of the other mutants examined, loss of the Tof1, Mre11, Rad50, and Sae2 proteins reduced class 1 events three- to

Table 2 Functional roles of proteins examined in this study

Protein	Enzymatic activity: pathway involvement in mitosis
Elg1p[a,b]	Subunit of replication factor C complex: involved in stability of replication fork, HR, and telomere maintenance
Rrm3p[b]	DNA helicase: relieves replication fork pauses at G4 motifs, tRNA genes, and other fork-stalling sequences
Sgs1p[b]	DNA helicase: involved in unwinding of HR intermediates and intermediates formed during DNA replication, unwinds G4 structures; in complex with Dna2p, Top3p, and Rmi1p promotes 5′-3′ resection
Srs2p[b]	DNA helicase: negative regulator of HR at replication fork, promotes resolution of HJs by Mus80p/Mms4p, unwinds triplet repeat hairpins
Tof1p[b]	Subunit of replication-fork-pausing complex: stabilizes replication fork and facilitates progression of fork to prevent genomic alterations; S-phase checkpoint function
Top1p[b]	Topoisomerase I: involved in DNA replication, recombination, and transcription
Exo1p[c]	5′–3′ exonuclease, flap-endonuclease: involved in processing of broken ends, DNA mismatch repair, error-free postreplication pathway, and telomere maintenance
Mre11p[c]	Nuclease subunit of Mre11p/Rad50p/Xrs2p complex: processing of DNA ends resulting from DSB, roles in HR and NHEJ, telomere maintenance, and checkpoint functions.
Mus81p[c]	Interacts with Mms4p to form structure-specific endonuclease: promotes reciprocal crossovers in HR pathway
Rad1p[c]	Single-stranded endonuclease: NER and SSA pathway of HR
Rad50p[c]	Part of complex with Mre11p/Xrs2p: processing of DNA ends resulting from DSB, roles in HR and NHEJ, telomere maintenance, and checkpoint functions.
Rad51p[c]	Strand-exchange protein: most HR pathways except SSA
Rad52p[c]	Stimulates Rad51p and anneals single-stranded DNA: all HR pathways
Rad59p[c]	Paralog of Rad52p: stimulates SSA
Sae2p[c]	Endo- and exonuclease: roles in resection needed at telomeres and at broken DNA ends for DSB repair by HR; removal of MRX complex from DNA ends
Sml1p[c]	Inhibitor of ribonucleotide reductase: DSB repair
Lig4p[d]	Specialized DNA ligase: NHEJ pathway
Mms2p[e]	Ubiquitin-conjugating enzyme: involved in error-free postreplication repair
Rad18p[e]	E3 ubiquitin ligase: postreplication repair
Rev3p[f]	Catalytic subunit of DNA polymerase ζ: error-prone bypass of lesions during DNA replication
Msh2p[g]	Mismatch-binding protein: DNA mismatch repair, processing of DNA branches in SSA pathway
Msh6p[g]	Mismatch-binding protein acting with Msh2p: Repair of base–base mismatches
Rif1p[h]	Rap1p-binding protein: mutant results in increased telomere silencing and elongated telomeres
Sir2p[h]	Histone deacetylase: regulates silencing at *HML*, *HMR*, telomeres, and rDNA; regulates life span, negative regulator of DNA initiation
Sir3p[h]	Silencing protein interacting with Rap1p and Sir2p: regulates silencing at *HML*, *HMR*, and telomeres, but not in rDNA
Tel1p[h]	Protein kinase: telomere length regulation and DNA damage checkpoint

DSB, double-strand break; HJ, Holliday junction; HR, homologous recombination; MRX, Mre11p/Rad50p/Xrs2p; NER, nucleotide excision repair; NHEJ, nonhomologous end-joining; SSA, single-strand annealing.

[a] The functions for these proteins were determined using data in the *Saccharomyces* Genome Database (https://www.yeastgenome.org).

[b] These proteins are involved in stabilization of the replication fork and mutants lacking these proteins have elevated rates of genome instability.

[c] The proteins directly or indirectly affect the repair of double-strand DNA breaks by homologous recombination.

[d] This enzyme is required for "classic" nonhomologous end-joining.

[e] These proteins are utilized in error-free postreplication repair.

[f] Rev3p is required in the error-prone pathway of postreplication repair.

[g] Both Msh2p and Msh6p are required for the repair of base–base mismatches.

[h] These proteins affect telomere length and/or telomere silencing.

eightfold (Table 1). Tof1p is involved in protein-mediated stalling at the replication fork (Hodgson *et al.* 2007) and may extend the length of the ITS stall caused by the binding of Rap1 and other telomere-binding proteins; loss of Tof1 also reduces the rate of expansions within the ITS (Aksenova *et al.* 2015). The MRX complex and Sae2p are involved in the processing of DNA ends, and cleavage of DNA hairpin intermediates *in vivo* is dependent on Sae2p and the MRX complex (Symington *et al.* 2014; Table 2). In addition, quadruplex structures involving the ITS could form a substrate for the Mre11 nuclease (Ghosal and Muniyappa 2005). We tested whether the nuclease activity of Mre11p stimulated class 1 events by examining the rate of these events in a strain with the *mre11-H125N* (nuclease-dead) allele. This mutation reduced class 1 events by about threefold (Table 1), indicating that class 1 events are partially dependent on this activity.

Since the *tof1* and *mre11* deletions lowered the rate of class 1 events, we also examined the rate of class 1 events in *tof1 mre11* double mutants. We found that the *tof1 mre11* strain had a rate of class 1 events that was similar to the *tof1* single mutant (Table 1). Although this result suggests that Mre11p and Tof1p may operate in the same pathway to promote class 1 events, this interpretation is complicated by the observation that *mre11* mutants themselves are strong mutators, elevating mutation rates ~10-fold (Huang *et al.* 2003). In addition, since both Tof1p and the MRX complex have multiple cellular roles, other interpretations of this result are also possible.

Mutations in both *sir2* and *sir3* reduced the rate of class 1 events twofold and 17-fold, respectively (Table 1). Although there are several possible interpretations of this result, we suggest that the Sir2 and Sir3 proteins, which bind to telomeres, may also bind to the ITS, inducing partial

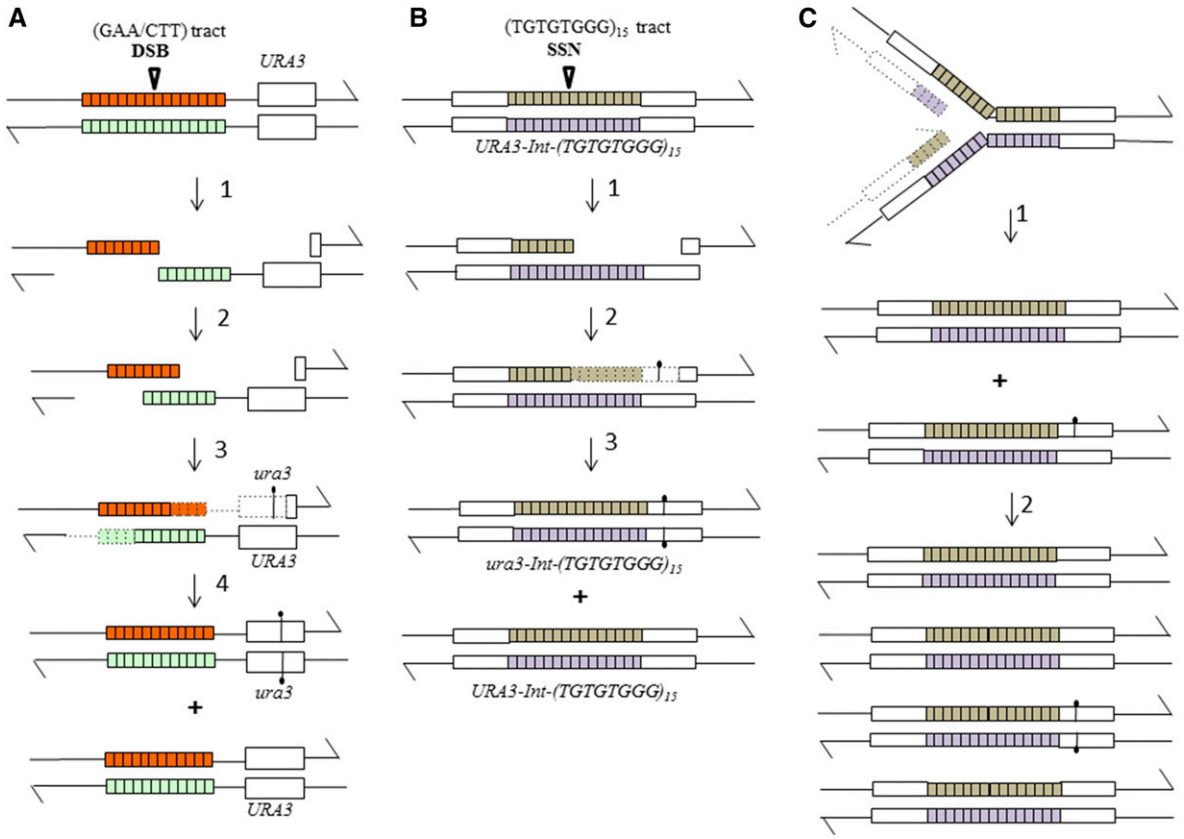

Figure 2 Point mutations induced within $(GAA)_N$ repeats and by ITSs. The chromosomes containing the repeats are shown as double-stranded DNA molecules with arrows marking the 3′ ends. In all of the proposed mechanism, the mutant base is introduced into only one strand of the duplex, and replication of the resulting DNA molecule produces one mutant gene and one wild-type gene. (A) Point mutations induced by $(GAA)_N$ repeats (Tang *et al.* 2013). As described in the text, $(GAA)_N$ tracts are frequently broken in both replicating and nonreplicating yeast cells. DSB formation, followed by 5′–3′ resection of the broken ends, results in products that can reanneal. Reannealing, followed by gap repair with an error-prone DNA polymerase ζ (Rev3p), could produce a mutation in one strand of the linked *URA3* gene. Replication of this product would result in one Ura^+ and one Ura^- cell. This mechanism would result in loss of (GAA) repeats. (B) Mutations introduced by single-stranded gap formation. We suggest that the ITS can be nicked by the Mre11p-associated endonuclease. This nick could be extended into a gap by the 3′–5′ Mre11p-associated nuclease and the 5′–3′ activities of Exo1p or Dna2-Sgs1-Top3p-Rmi1 complex. The resulting gap is filled in by the Rev3p-associated error-prone DNA polymerase. This process could occur outside of the S-period or be associated with a stalled replication fork. No alteration in the size of the ITS is expected from this mechanism. (C) Mutations introduced in the absence of a DNA lesion. In this model, the error-prone DNA polymerase is recruited to a stalled replication fork in the absence of a DNA lesion. This type of recruitment has been observed to be associated with certain DNA polymerase mutations (Northam *et al.* 2010). DSB, double-strand break; ITS, interstitial telomeric sequence.

silencing. This partial silencing may contribute to fork stalling at the ITS. If fork stalling is reduced in the *sir2* and *sir3* mutants, the MRX complex and DNA polymerase ζ may be recruited less often, resulting in a lower level of ITS-associated mutations. We note that the postulated binding of Sir2p and Sir3p to the ITS is not sufficient to turn off expression of the *URA3* reporter gene or *TRP1* gene; however, the expansion of the ITS that occurs in class 2 strains does silence *TRP1* expression (Aksenova *et al.* 2013).

Loss of the Rad52p resulted in a fourfold elevation of class 1 events. Previously, *rad52* strains have been shown to have a strong global mutator phenotype (Huang *et al.* 2003), likely reflecting the channeling of the repair of DNA lesions from the error-free HR pathway to error-prone pathways (Kunz *et al.* 1989). As expected from this model, the *rad52* mutation also substantially decreased the level of class 2 events, as will be discussed in detail in the next section.

None of the other mutants examined had a strong effect on the rate of class 1 alterations. Although the lack of effect of the mismatch repair (MMR) mutations *msh2* and *msh6* may seem surprising, the mutator phenotype of these strains in our genetic background at the *CAN1* locus is small (sixfold elevation in rates in the *msh2* strain AM24 compared to the wild-type strain PG329) compared to the 100-fold stimulation of mutations by the ITS. This result is consistent with the Rev3-dependence of class 1 events, since the mismatch repair system fails to efficiently correct mutations caused by DNA polymerase ζ (Lehner and Jinks-Robertson 2009). In summary, our analysis suggests that the ITS stimulates point mutations by a mechanism that may involve an endonucleolytic nick of the ITS, followed by gap formation and recruitment of the error-prone DNA polymerase ζ. A further description of this model, including various caveats, will be given in the *Discussion*.

Genetic regulation of class 2 events

Class 2 events represent HR between the ITS and the left telomere. Most mitotic recombination events are likely initiated by DSBs, although some events appear to be initiated by single-strand nicks or gaps (Symington *et al.* 2014). The genetic regulation of class 2 events is likely to be more complicated than for class 1 events for several reasons. First, these events reflect the interaction between two substrates, the ITS and the telomere, rather than an event triggered solely by the ITS. Second, most HR pathways involve multiple steps (end resection, strand invasion, and junction resolution), each step requiring multiple proteins (Symington *et al.* 2014). For these reasons, we expected to find many genes that would reduce or elevate the rate of class 2 events.

Before discussing the effects of individual mutations, we should emphasize that the rate of class 2 events can be regulated either by affecting the rate of DSB formation or by affecting the efficiency with which a DSB is processed to yield a terminal inversion. In regard to the second point, a DSB within the ITS has at least four potential fates (Figure 3): (a) repair of the DSB to produce a terminal inversion, (b) rejoining of the broken ends by reannealing the ITSs, thus restoring the original arrangement of chromosomal sequences, (c) repair of the DSB utilizing the sequences on the sister chromatid, or (d) Failure to repair the DSB, leading to cell death. Since we can assay only the first of these four pathways, a mutation that alters the rate of one of the three undetectable pathways may indirectly affect the rate of the terminal inversions. This issue will be discussed further below.

The *lig4* mutation that eliminates nonhomologous end-joining had no effect on the rate of class 2 events, whereas mutations in the HR pathway (*MRE11*, *RAD50*, *RAD52*, and *RAD59*, but not *RAD51*) reduced the rate of these events (Table 1). The lack of an effect of the *rad51* mutation, in contrast to the effects of the *rad52* and *rad59* mutations, strongly argues that the terminal inversions reflect SSA (Symington *et al.* 2014). SSA is usually assayed by inducing a DSB in single-copy sequences located between two direct repeats (Figure 4A). Following end resection, the complementary sequences of these repeats anneal. Since this process involves annealing, but not strand invasion, Rad52p, but not Rad51p, is required (Ivanov *et al.* 1996). The single-stranded branches of the intermediate are removed by the Rad1, Rad10, Msh2, and Msh3 proteins (Symington *et al.* 2014). We suggest that class 2 events are generated by a similar process (Figure 4B). As expected from this model, the rate of class 2 events is significantly reduced by *rad1* or *msh2* mutations (Table 1). The structure-specific nuclease Mus81p has no role in the SSA pathway and, as expected, had no effect on the rate of class 2 events (Table 1).

The 7–10-fold reduction in rates of class 2 events in the *mre11* and *rad50* strains could reflect either a role of the MRX complex in DSB formation at the ITS or the role of these proteins in end resection. However, since the nuclease-dead *mre11-H125N* allele does not reduce levels of class 2 events, the MRX complex is unlikely to be directly involved in making the DSB. Similarly, the lack of effect of the *sae2* mutation suggests that the nuclease activity of Mre11p does not contribute to DSB formation at the ITS. An alternative possibility is that the MRX complex is involved at a subsequent step in generating class 2 events. The MRX complex has a structural role in bridging DNA ends, and this function is deficient in *mre11*Δ strains but unaffected in *mre11-H125N* strains (Lobachev *et al.* 2004). We suggest that the MRX complex may stabilize the intermediate in which the ITS and telomeric sequences are paired, facilitating the subsequent steps in SSA. Since the SSA event that generates class 2 events involves a very small ($\leq$ 120 bp) heteroduplex relative to the gene-sized regions of heteroduplex analyzed in most studies (Figure 4), the MRX-mediated stabilization of the intermediate may be important. A second relevant observation is that the Mre11p has DNA unwinding activity that is independent of its nuclease activity (Ghodke and Muniyappa 2013). This unwinding activity may facilitate the SSA pathway.

Mutants lacking Tof1p had about a twofold reduction of class 2 events. As described for the class 1 events, since *tof1* mutants reduce stalling caused by proteins bound at ITSs (Anand *et al.* 2012), there may be a lower level of ITS-associated DSBs, leading to a reduced rate of class 2 events. We also examined a *tof1 mre11* double-mutant strain. 0/41 5-FOA^R strains had class 2 events in this strain (Table S4). This low rate likely reflects a lower rate of DSB formation (because of *tof1*) coupled with a defect in stabilizing the interaction between the telomere and the ITS (because of *mre11*), as described above.

As described above, loss of Sir2p or Sir3p resulted in a reduction in class 1 events. In contrast, loss of Sir2p elevated the rate of class 2 events threefold; loss of Sir3p had no effect on class 2 events. One difference between these two silencing proteins is that Sir2p, unlike Sir3p, affects silencing in the ribosomal DNA (Gartenberg and Smith 2016). It is likely that the elevation in class 2 events is not ITS-specific. Foss *et al.* (2017) reported that loss of Sir2p resulted in increased replication gaps in the genome and suggested that the activation of ribosomal DNA replication origins in *sir2* strains results in less efficient replication of other genomic sequences. They found a three- to fivefold elevation in mitotic recombination in non-rDNA sequences, consistent with the threefold elevation of class 2 events in the *sir2*, but not the *sir3*, strain.

Strains lacking Rrm3p, Sgs1p, or Srs2p had rates of class 2 events that were three- to fivefold less than wild-type strains; mutants lacking Mms2p or Rad18p [components of the post-replication repair (PRR) pathway] had no significant effect on the rates of class 1 or class 2 events (Table 1). Sgs1p, Srs2p, and Rrm3p are all helicases, and Sgs1p and Srs2p are antirecombinases (Symington *et al.* 2014). One interpretation of our observations is that loss of these proteins elevates the frequency of sister-chromatid exchange (Figure 3C), thereby reducing DSB repair in the competing terminal inversion pathway (Figure 3A) responsible for class 2 events. Since the SSA pathway does not involve Rad51p or formation of a Holliday junction, the

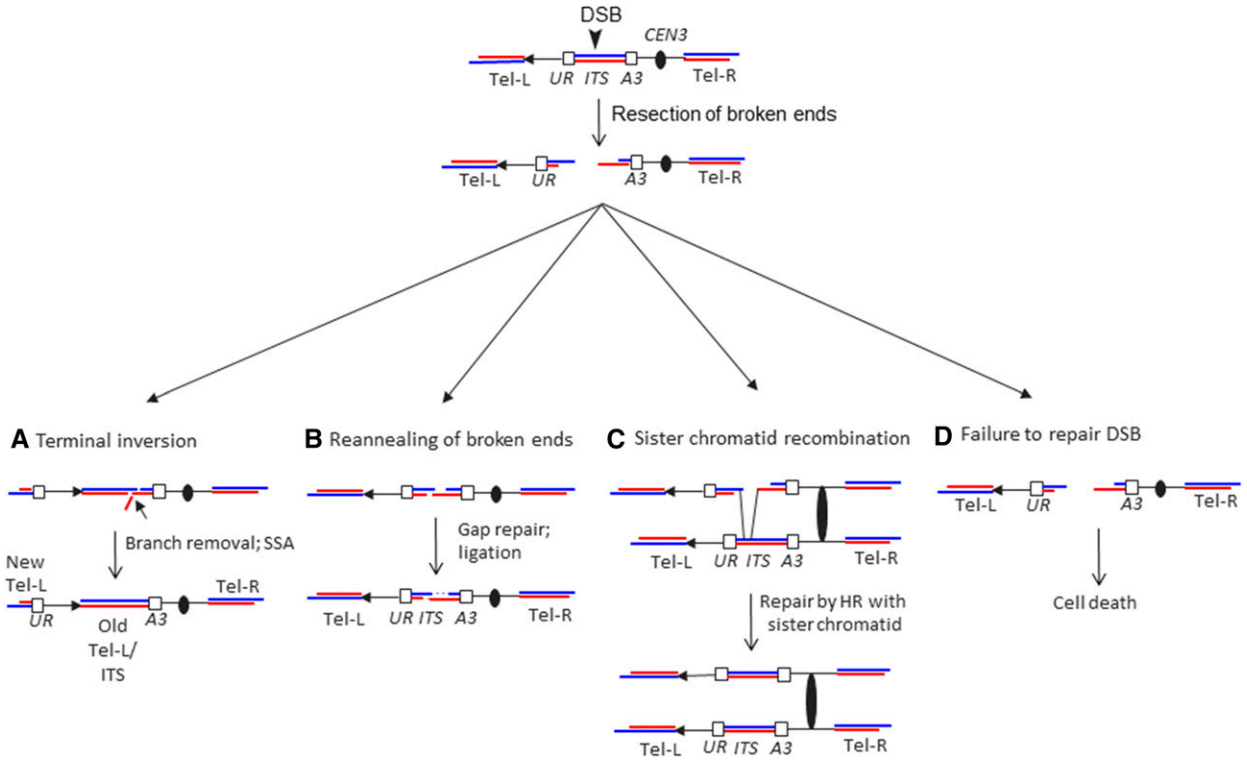

Figure 3 Mechanisms for the repair of a DSB in the *URA3-Int-*$(TGTGTGGG)_{15}$ reporter gene. As in Figure 1, the CA-rich and GT-rich telomeric strands are shown in red and blue, respectively. All products are initiated by a DSB within the ITS, followed by 5′–3′ resection of the broken ends. A horizontal arrow indicates the orientation of the chromosomal segment between the left telomere and the reporter gene. (A) Repair of a DSB resulting in terminal inversion. Following processing of the broken ends, the left telomere could undergo an SSA event with the centromere-proximal broken end to generate the inversion. Since the telomeric tract is longer than the ITS, the reannealed intermediate is likely to contain a single-stranded DNA branch that would require Msh2p/Msh3p/Rad1p/Rad10p for its removal. The cell with this rearrangement would be 5-FOA^R. (B) Reannealing of broken ends. If the repair event does not involving the flanking *URA3* coding sequences, this mechanism would not be expected to produce a 5-FOA^R derivative. (C) Repair of DSB by sister chromatid recombination. As in (B), this mechanism would not result in a 5-FOA^R derivative. (D) Failure to repair the DSB. If the ITS-associated DSB is not repaired, the centromere-containing fragment would lack a telomere and would be lost, leading to cell inviability. 5-FOA^R, 5-FOA-resistant; DSB, double-strand break; HR, homologous recombination; ITS, interstitial telomeric sequence; SSA, single-strand annealing.

antirecombinase activities of Sgs1p and Srs2p would not be likely to affect the rate of terminal inversions directly.

The lowered rate of class 2 events in the *rrm3* strain was quite unexpected. Since Rrm3p promotes replication fork progress through ITSs and other hard-to-replicate sequences (Ivessa *et al.* 2002), we expected that loss of Rrm3p would lead to elevated DSB formation in the ITS and increased formation of the terminal inversion. However, Muñoz-Galván *et al.* (2017) showed recently that Rrm3p is required for the repair of broken replication forks. Although most of these studies concerned sister-chromatid recombination, it is possible that SSA is also stimulated by Rrm3p. Thus, loss of Rrm3p would result in elevated cell death (Figure 3D) and a reduced rate of class 2 events (Figure 3A).

Loss of Tel1p elevated terminal inversions about threefold. It is possible that recruitment of telomerase to telomeric repeats results in less efficient SSA. Since Tel1p is involved in recruiting telomerase to the telomeres, loss of Tel1p could allow more efficient SSA. It is unlikely that the short telomeres characteristic of *tel1* strains (Lustig and Petes 1986) contribute directly to elevated rates of class 2 events. The *mre11* and *rad50* strains have equally short telomeres and a reduced level of class 2 events (as described above), and the *rif1* mutation that results in extended telomeres (Hardy *et al.* 1992) had no significant effect on class 2 events (Table 1). In addition, mutants that lacked Elg1p (involved in stabilizing the replication fork), Top1p (topoisomerase I), and Sml1p (an inhibitor of ribonucleotide reductase) had no substantial effects on either class 1 or 2 events (Table 1).

Effects of hydroxyurea on the rates of ITS-induced genomic alterations

ITSs are associated with replication fork stalling and *tof1* mutants reduce fork stalling (Anand *et al.* 2012); we found that the *tof1* mutation reduced the rates of both class 1 and 2 events. Hydroxyurea (HU) reduces the pools of deoxyribonucleotides, resulting in an accumulation of single-stranded DNA at the replication fork and triggering of a Mec1p-dependent DNA damage checkpoint (Signon 2018). Although the reduction in DNA fork movement caused by HU might be expected to increase the rate of fork stalling, we previously showed that HU reduced fork stalling at ITSs (Anand *et al.*

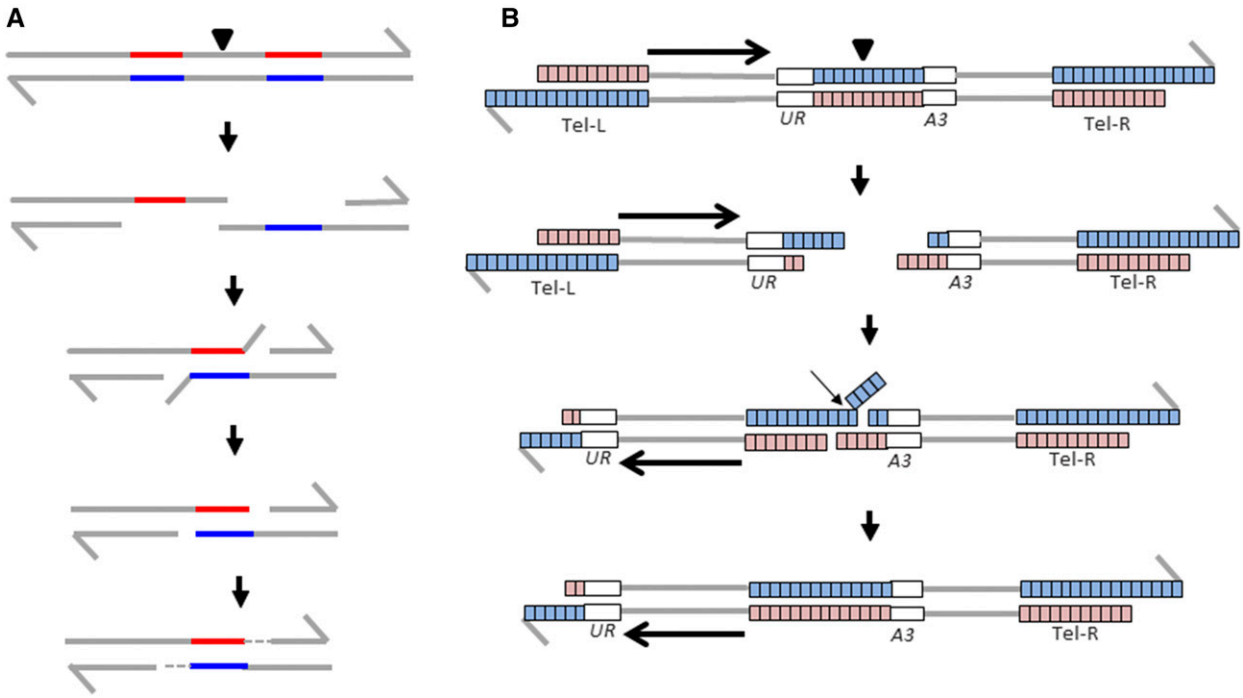

Figure 4 SSA as the mechanism for producing class 2 events. Each chromosome is shown as a double-stranded molecule. (A) "Classic" SSA. SSA is often analyzed in strains that have two closely-linked directly repeated genes separated by an HO or I-*Sce*I site (Symington *et al.* 2014). Following DSB formation (shown by the arrow), the broken ends are resected and pairing occurs between the nonallelic repeats. The resulting single-strand branches are removed by the Rad1p/Rad10p/Msh2p/Msh3p enzymes and the gaps are filled in by DNA polymerase. (B) SSA as a mechanism for producing a class 2 event. Following DSB formation within the ITS, the broken ends are resected, allowing pairing between the left telomere and the centromere-containing DNA fragment. This pairing process requires Rad52p and is aided by Rad59p, but is independent of Rad51p. Following reannealing, single-stranded branches are removed as in (A) and the resulting gaps filled in by DNA polymerase. DSB, double-strand break; SSA, single-strand annealing.

2012). To determine whether HU affected genomic rearrangements, we compared the rates of class 1 and 2 events in the wild-type PG329 strain grown in the presence (100 mM) and absence of HU. The results are shown in Table S5.

HU significantly elevated the rate of class 1 alterations and significantly reduced the rate of class 2 alterations. The elevated rate of class 1 alterations could be explained by an increased efficiency of recruitment of DNA polymerase ζ to the large single-stranded regions at the replication fork in HU-treated cells. Alternatively, the reduced pools of deoxyribonucleotides could result in the increased misincorporation of nucleotides by the replicative DNA polymerases or by DNA polymerase ζ. To determine whether the elevation in point mutations in HU-treated cells was specific to the reporter gene containing the ITS, we examined the rate of class 1 events in a strain (MD737) in which the *URA3* reporter gene lacked the ITS. HU resulted in a fourfold elevation in mutation rates, indicating that the effects of HU are independent of the ITS. Northam *et al.* (2010) previously reported that HU (100 mM) elevated the frequency of *CAN1* mutations by about eightfold, and that the increase was largely dependent on Rev3p. Thus, the elevation of class 1 events reflects mutagenic effects that are independent of the ITS.

Although HU was reported to elevate the rate of reciprocal mitotic crossovers ~40-fold in one assay (Barbera and Petes 2006), the rate of class 2 events was reduced about eightfold by HU (Table S5). This reduction is consistent with the fivefold decrease in fork stalling at the ITS in the presence of HU observed by Anand *et al.* (2012). It is also possible that the lower pools of deoxyribonucleotides in cells treated with HU reduce the efficiency of some steps in SSA. Finally, since the HU-induced DNA damage could result in elevated global cohesion of sister chromatids (Unal *et al.* 2007), this cohesion would be expected to produce more efficient repair of the DSB by sister-chromatid recombination. As shown in Figure 3, more efficient repair of a DSB by sister-chromatid recombination might then reduce the observed rate of terminal inversions, although other possibilities cannot be excluded.

Discussion

Below, we will summarize the mechanisms by which the ITSs produce class 1 and 2 events, as well as caveats associated with these proposed mechanisms. We will also compare our results with previous studies of ITSs in yeast and mammalian cells.

Molecular mechanisms that result in class 1 and 2 events

Although the ITS stimulates both point mutations and terminal inversions, these two types of events are regulated quite differently. The point mutations are dependent on the error-prone DNA polymerase ζ. Since the size of the ITS did not decrease in strains with the point mutation, these mutations are not likely to be a consequence of the mutagenic repair of a DSB. Instead, we suggest that the mutations are introduced during repair of a single-stranded gap (Figure 2B and Figure 5A). Since class 1 events are reduced in strains lacking Mre11p, Rad50p, and Sae2p (which activates the Mre11p nuclease), or containing the nuclease-deficient *mre11-H125N* allele, the proposed gap may be initiated by a nick caused by the Mre11p endonuclease that is expanded into a gap by the 3′–5′ nuclease of Mre11p, and the 5′–3′ activities of Exo1p or Sgs1p/Top3p/Rmi1p/Dna2p (Symington *et al.* 2014). We found that mutations in neither *EXO1* nor *SGS1* reduced the rate of class 1 events (Table 1), possibly due to the redundancy of the enzymes involved in resection.

Unlike the class 1 events, the class 2 events are likely initiated by a DSB. In a previous study with an ITS that was about twice as long as that used in our study, Goto *et al.* (2015) found an ITS-associated DSB. In contrast to class 1 events, class 2 events occurred independently of the nuclease activity of Mre11p. As with most other spontaneous mitotic recombination events, the enzymes that initiate DSB formation at the ITS are not known. In addition, although the partial dependence of class 2 events on Tof1p argues that about half of the DSBs may be associated with stalled replication forks, about half of these events may be independent of DNA replication. Previously, we showed that more than half of spontaneous mitotic crossovers in yeast are associated with DSB formation in unreplicated chromosomes (Lee *et al.* 2009; St. Charles and Petes 2013). In addition, Zhang *et al.* (2012) showed that tracts of GAA/TTC repeats simulated DSBs in both S-phase and in nondividing cells.

Following the initiating DNA lesion, the subsequent steps in the generation of class 2 events have the same genetic requirements as SSA (Figure 5B). Rad51p is dispensable for an SSA event, presumably because heteroduplex formation occurs between two single-stranded DNA ends without the requirement for strand invasion. As observed in previous studies of "classic" SSA (Davis and Symington 2001), we found that a lack of Rad52p reduced the rate of class 2 events more severely than the loss of Rad59p (Table 1). Rad59p interacts with Rad52p to stimulate SSA (Davis and Symington 2001).

Caveats about the proposed mechanisms of class 1 and 2 events

Although the Rev3p-dependence of class 1 events and the reliance of class 2 events on the SSA pathway are clear, there are a number of mutations that had effects with multiple possible interpretations. For example, we suggested that the elevation of class 2 events in strains lacking Sir2p might be an indirect effect of the replication stress imposed by the unsilencing of replication origins in the ribosomal DNA, leading to elevated DSB formation. However, since Sir2p is a histone deacetylase with multiple potential targets, other possibilities also exist. Aksenova *et al.* (2015) noted that the *sir2* mutation resulted in a 26-fold elevation in tract expansions of the ITS.

In our study of ITS-induced alterations, most of the mutations had relatively small effects, affecting the rate of the events < 10-fold. In contrast, in studies of recombination events induced by site-specific meganucleases such as HO or I-*Sce*I, mutations often have larger quantitative effects. For example, loss of Rad52p reduces the efficiency of HO-induced recombination by 100-fold (Malkova *et al.* 1996) but has only a 10-fold effect on class 2 events. One difference between spontaneous events and those induced by meganucleases is that meganucleases produce a single type of DNA lesion, whereas spontaneous events likely reflect multiple types of DNA lesions. Thus, there are likely to be a large number of pathways that are relevant to the repair of spontaneous DNA damage. Some of these pathways may be redundant such that eliminating any single pathway has a relatively small effect.

Genetic regulation of ITS-induced alterations in other studies

In the current study, the ITS is oriented such that the G-rich telomeric repeats are on the Watson strand, as defined in the *Saccharomyces* Genome Database (Figure 1). In another study, we analyzed genomic alterations in strains with the reverse orientation of the ITS (Aksenova *et al.* 2015). In this orientation, strains with the *URA3*::*Int* $(ACACACCC)_{15}$ allele are 5-FOA^R. However, strains with only eight copies of the telomere repeat [*URA3*::*Int* $(ACACACCC)_8$] have a leaky Ura$^-$ phenotype and grow weakly on medium containing 5-FOA. Fast-growing 5-FOA^R derivatives have expansions of the telomeric tract. These expansions are dependent on two recombination pathways that both require Rad6p: a gap-repair pathway requiring the HR proteins Rad51p and Rad52p, and a PRR pathway utilizing Rad5p. We previously suggested that telomeric proteins bound to the ITS result in fork stalling and a Tof1p-mediated pause. This pause then facilitates template switching (PRR pathway) or gap filling (HR pathway). Since class 1 and class 2 events in our study are independent of Rad51p and the PRR proteins Mms2p and Rad18p, the mechanisms that generate class 1 and 2 events are clearly quite different from those that produce expansions of the ITS.

As discussed in the *Introduction*, ITSs in mammalian cells are often associated with fragile sites and with breakpoints of translocations observed in tumor cells. Although these observations suggest that ITSs stimulate DNA breaks, the alternative possibility is that ITSs get inserted at regions that are prone to breakage for other reasons. Our results, as well as several previous yeast studies (Aksenova *et al.* 2013, 2015; Goto *et al.* 2015), show that ITSs in yeast are themselves prone to generating chromosome rearrangements. Although the genetic regulation of ITS-caused instability in mammalian systems has not been examined in detail, Bosco and de

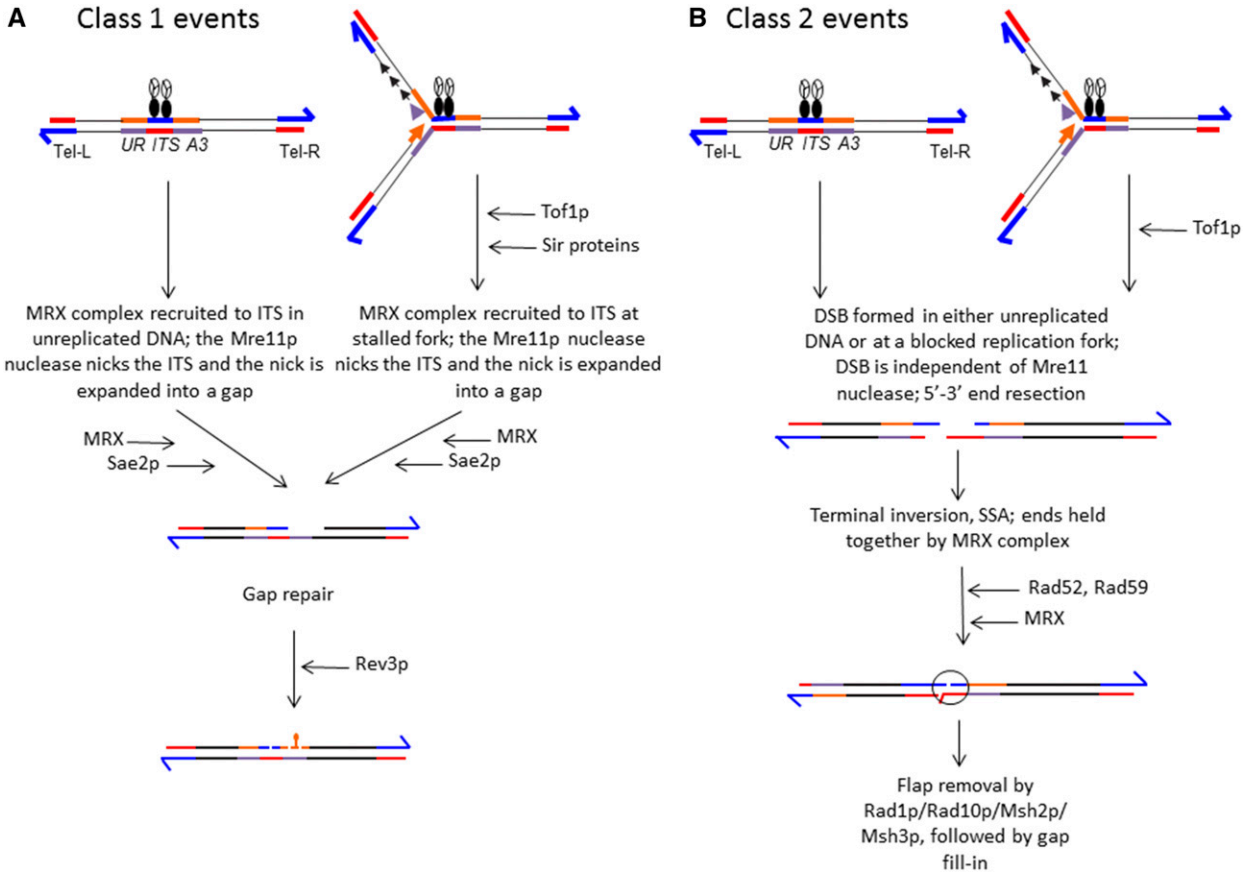

Figure 5 Summary of mechanisms that result in class 1 and 2 events. As in previous figures, blue and red lines show the G-rich and C-rich telomeric sequences, respectively. The black circles are the telomere-binding Rap1 proteins and the three-component circle is a complex of Sir2-4. The *URA3* coding sequences are shown as paired orange and purple lines. The reporter gene is replicated from an origin (*ARS306*) located to the left of the reporter. We suggest that many of the events are initiated by a replication fork block caused by the binding of telomere proteins to the ITS. The strength of the block is enhanced by Tof1p, since mutants of Tof1p lower the frequency of instability. The suppressing and enhancing effects of various proteins are shown as "T-bars" and horizontal arrows, respectively. For both classes of event, we suggest that the event may be initiated in unreplicated DNA or at a stalled fork. (A) Class 1 event. We hypothesize that the nuclease activity of the MRX complex creates a nick in either unreplicated DNA or at a stalled replication fork. This stall may be promoted by Tof1p and the Sir proteins. Formation of the nick requires Sae2p, which activates the Mre11p nuclease. The nick is expanded into a gap. The gap is filled in by the error-prone Rev3p DNA polymerase, resulting in a mutation in one strand of the *URA3* gene. Replication of this molecule would produce one chromosome with a *ura3* mutation and one with a wild-type *URA3* gene. (B) Class 2 event. Most of the details of this pathway are given in the text. In brief, the ITS undergoes a DSB in either unreplicated DNA or at a blocked replication fork. Tof1p enhances the efficiency of the block. Following resection of the broken ends, the left telomere anneals to the centromere-containing broken end. We suggest that this annealing is stabilized by the MRX complex. The annealing requires Rad52p and is enhanced by Rad59p. Subsequent removal of single strands requires Rad1p and Msh2p, and likely also involves Rad10p and Msh3p. DSB, double-strand break; ITS, interstitial telomeric sequence; MRX, Mre11p/Rad50p/Xrs2p.

Lange (2012) showed that deletion of the telomere-binding TRF1 protein elevated the fragility of an ITS in human cells.

Conclusions

In conclusion, our data strongly argue several points. First, the ITS-induced point mutations are initiated by a mechanism that is different from point mutations initiated by the trinucleotide tract GAA/CTT. Although the mutagenic effects of both types of sequence require Rev3p, the GAA/CTT tracts induce mutations by repair of a DSB, whereas the ITS induces mutations independently of a DSB, likely utilizing a Mre11p-generated single-strand gap. Second, class 2 events occur through the SSA pathway by a mechanism that requires the MRX complex but does not require the Mre11p-encoded nuclease.

Acknowledgments

We thank Ted Slotkin for advice about the statistical analysis, Catherine Freundenreich for comments on the manuscript, and Sue Jinks-Robertson and Lorraine Symington, as well as all members of the Petes and Jinks-Robertson laboratories, for useful discussions and comments on the manuscript. The research was supported by National Institutes of Health (NIH) grants R01 GM-24110, R01 GM-52319, and R35 GM-118020 to T.P., and R01 GM-60987 and P01 GM-105473 to S.M. A.Y.A. was supported by a Russian foundation for Basic Research grant (15-04-08658) and a research project in the Center for Molecular and Cell Technologies (Research Part, Saint Petersburg State University,

Russia). A.M. was supported by NIH grant 5T32 GM-007754-37.

Literature Cited

Aksenova, A. Y., P. W. Greenwell, M. Dominska, A. A. Shishkin, J. C. Kim *et al.*, 2013 Genome rearrangements caused by interstitial telomeric sequences in yeast. Proc. Natl. Acad. Sci. USA 110: 19866–19871. https://doi.org/10.1073/pnas.1319313110

Aksenova, A. Y., G. Han, A. A. Shishkin, K. V. Volkov, and S. M. Mirkin, 2015 Expansion of interstitial telomeric sequences in yeast. Cell Rep. 13: 1545–1551. https://doi.org/10.1016/j.celrep.2015.10.023

Anand, R. P., K. A. Shah, H. Niu, P. Sung, S. M. Mirkin *et al.*, 2012 Overcoming natural replication barriers: differential helicase requirements. Nucleic Acids Res. 40: 1091–1105. https://doi.org/10.1093/nar/gkr836

Azzalin, C. M., E. Mucciolo, L. Bertoni, and E. Giulotto, 1997 Fluorescence in situ hybridization with a synthetic (T2AG3)n polynucleotide detects several intrachromosomal telomere-like repeats on human chromosomes. Cytogenet. Cell Genet. 78: 112–115. https://doi.org/10.1159/000134640

Azzalin, C. M., S. G. Nergadze, and E. Giulotto, 2001 Human intrachromosomal telomeric-like repeats: sequence organization and mechanisms of origin. Chromosoma 110: 75–82. https://doi.org/10.1007/s004120100135

Barbera, M. A., and T. D. Petes, 2006 Selection and analysis of spontaneous reciprocal mitotic crossovers in *Saccharomyces cerevisiae*. Proc. Natl. Acad. Sci. USA 103: 12819–12824. https://doi.org/10.1073/pnas.0605778103

Bitterman, K. J., R. M. Anderson, H. Y. Cohen, M. Latorre-Esteves, and D. A. Sinclair, 2002 Inhibition of silencing and accelerated aging by nicotinamide, a putative negative regulator of yeast Sir2 and human SIRT1. J. Biol. Chem. 277: 45099–45107. https://doi.org/10.1074/jbc.M205670200

Boeke, J. D., F. Lacroute, and G. R. Fink, 1984 A positive selection for mutants lacking orotidine-5′-phosphate decarboxylase activity in yeast: 5-fluoro-orotic acid resistance. Mol. Gen. Genet. 197: 345–346. https://doi.org/10.1007/BF00330984

Bosco, N., and T. de Lange, 2012 A TRF-controlled common fragile site containing interstitial telomeric sequences. Chromosoma 121: 465–474. https://doi.org/10.1007/s00412-012-0377-6

Davis, A. P., and L. S. Symington, 2001 The yeast recombinational repair protein Rad59 interacts with Rad52 and stimulates single-strand annealing. Genetics 159: 515–525.

Foss, E. J., U. Lau, E. Dalrymple, R. L. Adrianse, T. Loe *et al.*, 2017 SIR2 suppresses replication gaps and genome instability by balancing replication between repetitive and unique sequences. Proc. Natl. Acad. Sci. USA 114: 552–557. https://doi.org/10.1073/pnas.1614781114

Gartenberg, M. R., and J. S. Smith, 2016 The nuts and bolts of transcriptionally silent chromatin in *Saccharomyces cerevisiae*. Genetics 203: 1563–1599. https://doi.org/10.1534/genetics.112.145243

Ghodke, I., and K. Muniyappa, 2013 Processing of DNA double-stranded breaks and intermediates of recombination and repair by *Saccharomyces cerevisiae* Mre11 and its stimulation by Rad50, Xrs2, and Sae2 proteins. J. Biol. Chem. 288: 11273–11286. https://doi.org/10.1074/jbc.M112.439315

Ghosal, G., and K. Muniyappa, 2005 Saccharomyces cerevisiae Mre11 is a high-affinity G4 DNA-binding protein and a G-rich DNA-specific endonuclease: implications for the replication of telomeric DNA. Nucleic Acids Res. 33: 4692–4703. https://doi.org/10.1093/nar/gki777

Goto, G. H., S. Zencir, Y. Hirano, H. Ogi, A. Ivessa *et al.*, 2015 Binding of multiple Rap1 proteins stimulates chromosome breakage induction during DNA replication. PLoS Genet. 11: e1005283. https://doi.org/10.1371/journal.pgen.1005283

Gottschling, D. E., O. M. Aparicio, B. L. Billington, and V. A. Zakian, 1990 Position effect at *S. cerevisiae* telomeres: reversible repression of Pol II transcription. Cell 63: 751–762. https://doi.org/10.1016/0092-8674(90)90141-Z

Greider, C. W., and E. H. Blackburn, 1985 Identification of a specific telomere terminal transferase activity in Tetrahymena extract. Cell 43: 405–413. https://doi.org/10.1016/0092-8674(85)90170-9

Guthrie, C., and G. R. Fink, 1991 *Guide to Yeast Genetics and Molecular Biology*. Academic Press, San Diego.

Hardy, C. F., L. Sussel, and D. Shore, 1992 A RAP-interacting protein involved in transcriptional silencing and telomere length regulation. Genes Dev. 6: 801–814. https://doi.org/10.1101/gad.6.5.801

Hodgson, B., A. Calzada, and K. Labib, 2007 Mrc1 and Tof1 regulate DNA replication forks in different ways during normal S phase. Mol. Biol. Cell 18: 3894–3902. https://doi.org/10.1091/mbc.E07-05-0500

Huang, M.-E., A.-G. Rio, A. Nicolas, and R. D. Kolodner, 2003 A genomewide screen in *Saccharomyces cerevisiae* for genes that suppress the accumulation of mutations. Proc. Natl. Acad. Sci. USA 100: 11529–11534. https://doi.org/10.1073/pnas.2035018100

Ivanov, E. L., N. Sugawara, J. Fishman-Lobell, and J. E. Haber, 1996 Genetic requirements for the single-strand annealing pathway of double-strand break repair in *Saccharomyces cerevisiae*. Genetics 142: 693–704.

Ivessa, A. S., J.-Q. Zhou, V. P. Schulz, E. K. Monson, and V. A. Zakian, 2002 Saccharomyces Rrm3p, a 5′ to 3′ DNA helicase that promotes replication fork progression through telomeric and subtelomeric DNA. Genes Dev. 16: 1383–1396. https://doi.org/10.1101/gad.982902

Kunz, B. A., M. G. Peters, S. E. Kohalmi, J. D. Armstrong, M. Glattke *et al.*, 1989 Disruption of the *RAD52* gene alters the spectrum of spontaneous *SUP4-o* mutations in *Saccharomyces cerevisiae*. Genetics 122: 535–542.

Kupiec, M., 2014 Biology of telomeres: lessons from budding yeast. FEMS Microbiol. Rev. 38: 144–171. https://doi.org/10.1111/1574-6976.12054

Lea, D. E., and C. A. Coulson, 1949 The distribution of the numbers of mutants in bacterial populations. J. Genet. 49: 264–285. https://doi.org/10.1007/BF02986080

Lee, P. S., P. W. Greenwell, M. Dominska, M. Gawel, M. Hamilton *et al.*, 2009 A fine-structure map of spontaneous mitotic crossovers in the yeast *Saccharomyces cerevisiae*. PLoS Genet. 5: e1000410. https://doi.org/10.1371/journal.pgen.1000410

Lehner, K., and S. Jinks-Robertson, 2009 The mismatch repair system promotes DNA polymerase zeta-dependent translesion synthesis in yeast. Proc. Natl. Acad. Sci. USA 106: 5749–5754. https://doi.org/10.1073/pnas.0812715106

Lin, K. W., and J. Yan, 2008 Endings in the middle: current knowledge of interstitial telomeric sequences. Mutat. Res. Mutat. Res. 658: 95–110. https://doi.org/10.1016/j.mrrev.2007.08.006

Lobachev, K., E. Vitriol, J. Stemple, and K. Bloom, 2004 Chromosome fragmentation after induction of a double-strand break is an active process prevented by the RMX repair complex. Curr. Biol. 14: 2107–2112. https://doi.org/10.1016/j.cub.2004.11.051

Lustig, A. J., and T. D. Petes, 1986 Identification of yeast mutants with altered telomere structure. Proc. Natl. Acad. Sci. USA 83: 1398–1402. https://doi.org/10.1073/pnas.83.5.1398

Makarova, A. V., and P. M. Burgers, 2015 Eukaryotic DNA polymerase zeta. DNA Repair (Amst.) 29: 47–55. https://doi.org/10.1016/j.dnarep.2015.02.012

Malkova, A., E. L. Ivanov, and J. E. Haber, 1996 Double-strand break repair in the absence of *RAD51* in yeast: a possible role for break-induced DNA replication. Proc. Natl. Acad. Sci. USA 93: 7131–7136. https://doi.org/10.1073/pnas.93.14.7131

Meyne, J., R. J. Baker, H. H. Hobart, T. C. Hsu, O. A. Ryder *et al.*, 1990 Distribution of non-telomeric sites of the (TTAGGG)n

telomeric sequence in vertebrate chromosomes. Chromosoma 99: 3–10. https://doi.org/10.1007/BF01737283

Muñoz-Galván, S., M. García-Rubio, P. Ortega, J. F. Ruiz, S. Jimeno *et al.*, 2017 A new role for Rrm3 in repair of replication-born DNA breakage by sister chromatid recombination. PLoS Genet. 13: e1006781. https://doi.org/10.1371/journal.pgen.1006781

Northam, M. R., H. A. Robinson, O. V. Kochenova, and P. A. Shcherbakova, 2010 Participation of DNA polymerase zeta in replication of undamaged DNA in *Saccharomyces cerevisiae*. Genetics 184: 27–42. https://doi.org/10.1534/genetics.109.107482

Northam, M. R., E. A. Moore, T. M. Mertz, S. K. Binz, C. M. Stith *et al.*, 2014 DNA polymerase zeta and Rev1 mediate error-prone bypass of non-B DNA structures. Nucleic Acids Res. 42: 290–306. https://doi.org/10.1093/nar/gkt830

Shah, K. A., and S. M. Mirkin, 2015 The hidden side of unstable DNA repeats: mutagenesis at a distance. DNA Repair (Amst.) 32: 106–112. https://doi.org/10.1016/j.dnarep.2015.04.020

Shah, K. A., A. A. Shishkin, I. Voineagu, Y. I. Pavlov, P. V. Shcherbakova *et al.*, 2012 Role of DNA polymerases in repeat-mediated genome instability. Cell Rep. 2: 1088–1095. https://doi.org/10.1016/j.celrep.2012.10.006

Signon, L., 2018 Genetic evidence for roles of yeast mitotic cyclins at single-stranded gaps created by DNA replication. G3 (Bethesda) 8: 737–752. https://doi.org/10.1534/g3.117.300537

St. Charles, J., and T. D. Petes, 2013 High-resolution mapping of spontaneous mitotic recombination hotspots on the 1.1 Mb arm of yeast chromosome IV. PLoS Genet. 9: e1003434. https://doi.org/10.1371/journal.pgen.1003434

Symington, L. S., R. Rothstein, and M. Lisby, 2014 Mechanisms and regulation of mitotic recombination in *Saccharomyces cerevisiae*. Genetics 198: 795–835. https://doi.org/10.1534/genetics.114.166140

Tang, W., M. Dominska, P. W. Greenwell, Z. Harvanek, K. S. Lobachev *et al.*, 2011 Friedreich's ataxia (GAA)n•(TTC)n repeats strongly stimulate mitotic crossovers in *Saccharomyces cerevisiae*. PLoS Genet. 7: e1001270. https://doi.org/10.1371/journal.pgen.1001270

Tang, W., M. Dominska, M. Gawel, P. W. Greenwell, and T. D. Petes, 2013 Genomic deletions and point mutations induced in *Saccharomyces cerevisiae* by the trinucleotide repeats (GAA·TTC) associated with Friedreich's ataxia. DNA Repair (Amst.) 12: 10–17. https://doi.org/10.1016/j.dnarep.2012.10.001

Unal, E., J. M. Heidinger-Pauli, and D. Koshland, 2007 DNA double-strand breaks trigger genome-wide sister-chromatid cohesion through Eco1 (Ctf7). Science 317: 245–248. https://doi.org/10.1126/science.1140637

Wellinger, R. J., and V. A. Zakian, 2012 Everything you ever wanted to know about *Saccharomyces cerevisiae* telomeres: beginning to end. Genetics 191: 1073–1105. https://doi.org/10.1534/genetics.111.137851

Wierdl, M., C. N. Greene, A. Datta, S. Jinks-Robertson, and T. D. Petes, 1996 Destabilization of simple repetitive DNA sequences by transcription in yeast. Genetics 143: 713–721.

Zhang, Y., A. A. Shishkin, Y. Nishida, D. Marcinkowski-Desmond, N. Saini *et al.*, 2012 Genome-wide screen identifies pathways that govern GAA/TTC repeat fragility and expansions in dividing and non-dividing yeast cells. Mol. Cell 48: 254–265. https://doi.org/10.1016/j.molcel.2012.08.002

Communicating editor: J. Surtees